Renewable Energy 256 (2026) 124643

Contents lists available at ScienceDirect

Renewable Energy

journal homepage: www.elsevier.com/locate/renene

Power take-off co-design and LCoE reduction of a hinged-type wave energy converter using a genetic algorithm

Zhijing Liao [b,a], Guang Li [a,*], Judith Apsley [a], Matteo F. Iacchetti [c,a], Peter Stansby [a]

[a] School of Engineering, The University of Manchester, Manchester, M13 9PL, UK
[b] Faculty of Mechanical and Electrical Engineering, Kunming University of Science and Technology, Kunming, China
[c] Department of Energy, Politecnico di Milano, Milan, Italy

ARTICLE INFO

Keywords:
Wave energy converter
Levelised cost of electricity
Co-design
Genetic algorithm

ABSTRACT

This paper addresses a power take-off (PTO) co-design problem of a wave energy converter (WEC), which is vital for the reduction of the levelised cost of electricity (LCoE). A genetic algorithm (GA) is employed to resolve this problem, with significant advantages over traditional methods. A hinged-type multi-float WEC M4 with an electrical drive train as its PTO is considered as a case study. Two key parameters for PTO design, the mechanical gearbox ratio and the generator rated torque, which have great impacts on both power capture of the WEC and the cost of the PTO, are selected as the co-design optimisation variables. The effectiveness of the proposed GA-based co-design approach is demonstrated, and its efficiency is quantified. Simulations using real sea data show that the proposed approach yields an optimal solution with significantly reduced LCoE. The proposed approach also has remarkably reduced computational load, approximately 1/3 compared with a benchmark line search method. The benefit of LCoE reduction can be more significant if more design parameters are considered. It is also found that up-scaling the WEC capacity also contributes to LCoE reduction. From 10 kW to 1 MW WEC capacity, LCoE can be reduced by a factor of 6.

1. Introduction

Wave energy is a competitive candidate for contributing to the future power supply, due to its high worldwide capacity [1] and availability [2]. For the past half century, many wave energy converter (WEC) designs have been proposed, which can be classified into several categories such as point-absorber, hinged, oscillating water columns (OWCs), cyclorotor types. There are also various types of power take-off (PTO) systems such as pneumatic, hydraulic, electric, as reviewed in [3]. To date, there is no definite answer on which combination of WEC and PTO provides minimum levelised cost of electricity (LCoE). It can only get clearer as researchers explore different technical routes more thoroughly.

A shared challenge for all types of WEC systems is the optimal design of subsystem parameters, e.g. WEC geometries, PTO components sizing, controller tuning, etc. Here we focus on the research problem of WEC PTO co-design, which aims to optimise the PTO design parameters for minimum LCoE of the WECs. In a traditional sequential design procedure, design parameters are treated disjointedly, which means design decisions made at former steps do not take into account dynamics and coupling effects from latter steps. This is not suitable for the design of WEC systems that have highly coupled hydro-dynamical, mechanical and electrical subsystems.

On the other hand, co-design approaches which follow a concurrent design strategy that considers multidisciplinary subsystem interactions from the beginning of the design process [4], are receiving increasing attention in the recent decade. In [5], a parametric control co-design approach is proposed to design the diameters of the turbine rotor and the bypass valve of an oscillating water column (OWC). The optimal control-informed design parameters are obtained by evaluating each possible combination of the design parameters in the parametric space, using a simplified LCoE performance function. In [6], a co-design method is proposed to design the optimal geometry of an oscillating-surge WEC to maximise electrical power generation. This is also done by sweeping through each possible width and height combinations in an iterative way. There are more WEC co-design studies such as [7, 8], but most of the existing WEC co-design approaches rely on a similar iterative line search strategy to determine the optimal design parameters. This is because WEC co-design optimisation problems are often discontinuous and non-convex, preventing the use of common optimisation solvers. However, this line search strategy introduces a

* Corresponding author.
E-mail addresses: zhijing.liao@manchester.ac.uk (Z. Liao), guang.li@manchester.ac.uk (G. Li), j.apsley@manchester.ac.uk (J. Apsley), matteo.iacchetti@manchester.ac.uk (M.F. Iacchetti), p.k.stansby@manchester.ac.uk (P. Stansby).

https://doi.org/10.1016/j.renene.2025.124643
Received 10 August 2024; Received in revised form 23 August 2025; Accepted 20 October 2025
Available online 6 November 2025

high computational burden, especially with a large number of design parameters, which is seldom mentioned or quantified in existing studies. A clear gap in knowledge is the lack of an effective and efficient method to resolve WEC co-design problems, without having to evaluate all possible combinations of design parameters in a burdensome way. Recently, the control co-design (CCD) of WECs, which considers interactions between controller and WEC design, has received increasing attention [9]. With CCD, the requirement of an efficient optimisation method is more exigent.

In this paper, we demonstrate how a genetic algorithm (GA) [10] can be applied to tackle WEC co-design problems and quantify its efficacy and computational burden in comparison to the iterative line search method. In the GA, design parameters are represented as 'genotype' and their performance is represented as 'phenotype' of an individual. A population is formed by individuals and evolves generation-by-generation based on the 'survival of the fittest' principle. In each generation, an evaluation-selection-reproduction process is followed. The GA outputs the best recorded individual and its 'genotype' (design parameters) when the number of generations reaches a pre-defined value.

As a case study, the GA is applied to resolve a typical co-design problem of a hinged-type multi-float WEC, called M4 [11], which uses an electrical drive train as its PTO. The kW-scale M4 has completed 6 months of sea trials at King George Sound, Albany, Australia [12–14]. Research on different aspects of the WEC-PTO system has been carried out, including WEC hydrodynamic modelling [12] and validation [15], PTO modelling [16], upper-level PTO torque control [17], and co-design which is the main focus here. Two key drive train parameters, the mechanical gearbox ratio and the rated torque of the generator are chosen as design parameters because the combination of these two parameters defines the torque–speed constraints of the WEC's operation which in turn influences power capture. At the same time, they are also closely linked to the cost of the PTO. A simplified LCoE fitness function is defined to guide the GA's evolution direction for deriving the optimal set of design parameters. A limitation to be pointed out here is this simplified LCoE assumes the PTO cost is a fixed 30% of the total capital cost of the WEC [18]. However, this should not affect the relative comparison of the proposed GA-based co-design algorithm and the traditional line search method. Simulation results indicate that the GA can effectively converge to an optimum design point and has a much lower computational burden in comparison to the traditional iterative line search method. For this two-variable co-design problem, the GA only requires 1/3 of the time needed by the line search method to yield the optimal parameters.

Finally, an estimation of LCoE reduction by up-scaling the WEC capacity is provided. This is based on Froude scaling of the optimum power capture obtained for the current 10-kW capacity device and estimations of the PTO cost at different capacities. A 20% reduction of power capture is assumed to take into account directional spreading waves. Cost of supercapacitor energy storage for power smoothing is also included, which is not considered when solving the co-design problem, assuming to be 20% more than the gearbox cost. With these assumptions, it is estimated at 1-MW capacity, the LCoE of M4 is approximately 1/6 of that for the current 10-kW capacity, which demonstrates a pathway for the cost reduction of wave energy.

The novelties and scientific contribution of this paper are summarised as follows:

- The genetic algorithm is applied to resolve a practical PTO co-design problem of a WEC for the first time. It is demonstrated that GA is effective and more efficient than the traditional line search method.
- The co-design results indicate that difference of the simplified LCoE between optimised and sub-optimal design parameters is huge, from over 4£/kWh to below 0.3£/kWh.
- Counter-intuitively, we found that design parameters that yield maximum power capture do not necessarily give minimum LCoE, which is an important finding for resolving WEC co-design problems in general.
- It is also found that the up-scaling of the WEC capacity can further benefit the LCoE reduction of WECs.

The remaining parts of this paper are structured as follows. Section 2 briefly introduces the WEC hydrodynamic model and the PTO model. Section 3 defines a simplified LCoE performance function. Section 4 details the two co-design approaches, the traditional line search method as a benchmark and the GA. Co-design results and comparisons are presented in Section 5 while conclusions are drawn in Section 6.

2. WEC and PTO models

2.1. The M4 hydrodynamic model

The M4 WEC for sea trial is shown in Fig. 1. It is about 21.3 m long and 9.5 m wide. There are, in total, four floats, one bow float connected rigidly with two middle floats and one stern float connected by beams to side-by-side hinges above the mid floats. When moored, from a single point mooring, the platform heads naturally into the wave direction due to wave drift forces. As waves propagate through the device, motions of the bow, mid and stern floats are out of phase to varying degrees, which causes the device to rotate about the hinges. The PTO is located at the hinges to generate electricity from the rotational motion. Note that the actual device for sea trial has two identical PTOs at the side-by-side hinges but here we consider this as a single PTO.

Linear diffraction/radiation methods based on potential flow theory have been used to model the dynamics of the platform in operational sea conditions [19], with similar configurations validated against experiment [11]. This is then converted into a control-oriented state-space form by system identification and model order reduction for rapid time-domain simulations. This state-space model is validated against the linear diffraction model [20] and shows high accuracy in predicting mean power capture of the M4 WEC. Readers are referred to [16,17] for more details on the state-space modelling. Here, the final state-space representation of the M4 hydrodynamic model is presented directly.

As power is mainly captured by the surge, heave and pitch motions, only model dynamics in these degrees of freedom (DOFs) are modelled. The motion vector can be defined as $\vec{\eta} = [x_0\ z_0\ \theta_l\ \theta_r]^\top$, where x_0 and z_0 are the surge and heave motion of the reference point at the centre of the hinges, θ_l is the relative pitch motion of the bow-mid float frame and θ_r is the relative pitch motion of the stern float, both with respect to the reference point at the hinges.

Based on Newton's Second Law of Motion, the equation of motion for the M4 WEC in the time domain based on Cummins method [21] for linear waves is

$$\boldsymbol{M}\ddot{\vec{\eta}}(t) = \vec{f}_{e,\eta}(t) + \vec{f}_{rd,\eta}(t) + \vec{f}_{rs,\eta}(t) + \vec{f}_{pto,\eta}(t) \tag{1}$$

where $\boldsymbol{M}$ is the 4 × 4 mass and inertia matrix. Here, $\vec{f}_{e,\eta}(t)$ is the wave excitation force, $\vec{f}_{rd,\eta}(t)$ is the radiation damping force, $\vec{f}_{rs,\eta}(t)$ is the hydrostatic restoring force and $\vec{f}_{pto,\eta}(t)$ is the PTO torque. Equations for modelling hydrodynamic forces can be found in [17]. Note that the mooring force is not modelled for simplification but a small stiffness term is added to the surge DOF to prevent model drift.

Eq. (1) can be further rewritten as

$$\begin{aligned}(\boldsymbol{M} + \boldsymbol{m}_\infty)\ddot{\vec{\eta}}(t) - \vec{f}_{rd,\eta}(t) - \vec{f}_{rs,\eta}(t) &= \vec{f}_{e,\eta}(t) + \vec{f}_{pto,\eta}(t)\\ \dot{\vec{z}}_s &= \boldsymbol{A}_s\vec{z}_s + \boldsymbol{B}_s\dot{\vec{\eta}}(t)\\ \vec{f}_{rd,\eta}(t) &= \boldsymbol{C}_s\vec{z}_s + \boldsymbol{D}_s\dot{\vec{\eta}}(t)\end{aligned} \tag{2}$$

where m_∞ is the 4 × 4 infinite-frequency added mass matrix and z_s is the auxiliary state of radiation subsystems with system matrices $\boldsymbol{A}_s$, $\boldsymbol{B}_s$, $\boldsymbol{C}_s$, $\boldsymbol{D}_s$ [22].

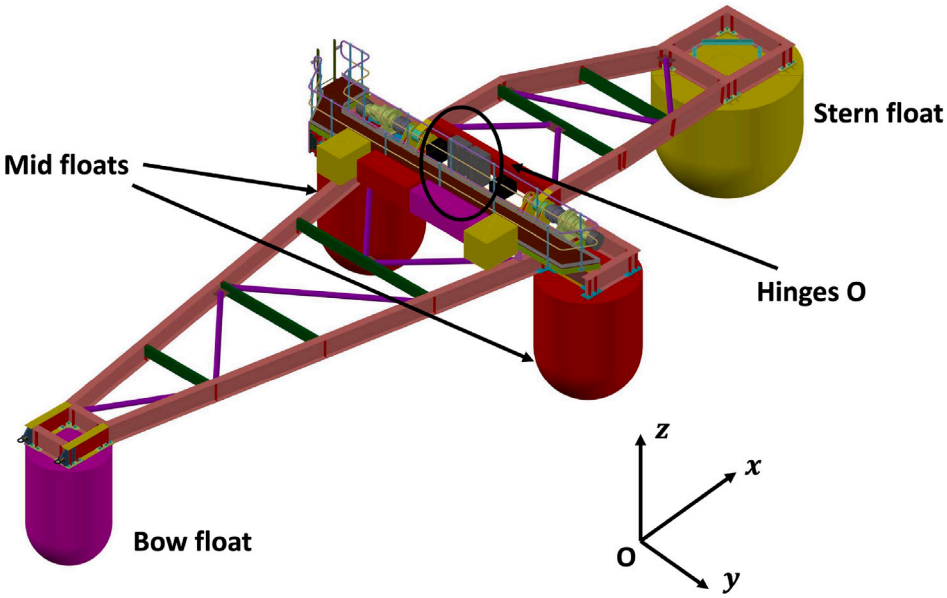

Fig. 1. The M4 1-2-1 design diagram, provided by BMT, Australia.

The PTO torque $\vec{f}_{pto,\eta}$ is provided by the PTO based on an upper-level WEC control algorithm.

$$\vec{f}_{pto,\eta}(t) = \begin{bmatrix} 0 \\ 0 \\ -T_\eta(t) \\ T_\eta(t) \end{bmatrix} \tag{3}$$

For demonstration purposes, the WEC control algorithm considered here is a simple passive damping controller, i.e.

$$T_\eta = -d_{pto}(\dot{\theta}_l - \dot{\theta}_r) \tag{4}$$

where d_{pto} is the damping ratio tuned for optimal power output and remains unchanged for PTO design, $\dot{\theta}_l - \dot{\theta}_r$ is the relative pitch velocity of the WEC's hinges.

By defining a new state vector $\vec{x} := [\vec{\eta}, \dot{\vec{\eta}}, \vec{z}_s]^\top$, the final linear state-space representation of the M4 WEC can be written as:

$$\begin{aligned} \dot{\vec{x}} &= \boldsymbol{A_c}\vec{x} + \boldsymbol{B_{wc}}\vec{f}_{e,\eta}(t) + \boldsymbol{B_{uc}}\vec{f}_{pto,\eta}(t) \\ y &= \boldsymbol{C_c}\vec{x} \end{aligned} \tag{5}$$

where the system matrices are

$$\begin{aligned} \boldsymbol{A_c} &= \begin{bmatrix} \boldsymbol{0}_{4\times4} & \boldsymbol{I}_{4\times4} & \boldsymbol{0}_{4\times n} \\ -(\boldsymbol{M}+\boldsymbol{m}_\infty)^{-1}\boldsymbol{K} & -(\boldsymbol{M}+\boldsymbol{m}_\infty)^{-1}\boldsymbol{D_s} & -(M+m_\infty)^{-1}\boldsymbol{C_s} \\ \boldsymbol{0}_{n\times4} & \boldsymbol{B_s} & \boldsymbol{A_s} \end{bmatrix} \\ \boldsymbol{B_{wc}} &= \begin{bmatrix} \boldsymbol{0}_{4\times4} \\ (\boldsymbol{M}+\boldsymbol{m}_\infty)^{-1} \\ \boldsymbol{0}_{n\times4} \end{bmatrix} \quad \boldsymbol{B_{uc}} = \begin{bmatrix} \boldsymbol{0}_{4\times1} \\ (\boldsymbol{M}+\boldsymbol{m}_\infty)^{-1}[0,0,-1,1]^\top \\ \boldsymbol{0}_{n\times1} \end{bmatrix} \\ \boldsymbol{C_c} &= \begin{bmatrix} \boldsymbol{0}_{1\times4} & [0\,0\,1\,-1] & \boldsymbol{0}_{1\times n} \end{bmatrix} \end{aligned} \tag{6}$$

Here $\boldsymbol{I}$ is the identity matrix and $\boldsymbol{0}$ is the matrix with zeros in all entries. $\boldsymbol{K}$ is the hydrostatic stiffness matrix. The size of $\boldsymbol{A_c}$ depends on the selected model order n for the radiation sub-system. The system output $y = \omega_\eta = \dot{\theta}_l - \dot{\theta}_r$ is the rotational velocity of the WEC's hinges.

This WEC hydrodynamic model in state-space form is the foundation for solving the WEC co-design problem. Even with an iterative line search approach, the state-space model enables rapid simulations run for estimating mechanical power generation under various irregular wave conditions. In the next subsection, the PTO model is introduced, which is used to construct torque–speed constraints for wave profile simulations and estimate power loss.

2.2. The PTO model

The M4 WEC uses an electrical drive train as its PTO. Key components of the drive train are briefly introduced here. Readers are referred to [16] for more details of the PTO specified for the M4 sea trial platform. The main intention here is to highlight why the gearbox ratio and the rated torque of the generator are selected as co-design parameters and how they influence the electrical power generation and ultimately the LCoE.

The electrical drive train consists of a mechanical gearbox, a permanent magnet synchronous generator (PMSG), an AC/DC converter to provide close-loop control of the PMSG's torque producing current. It also encompasses other important power electronic components, such as a DC/DC converter for DC voltage regulation, supercapacitors for power smoothing and a further DC/AC converter for grid interfacing. This is simplified for the clear presentation of the PTO co-design problem, keeping only the most cost-related components. A schematic diagram of the simplified PTO model used for WEC co-design is shown in Fig. 2 with the two design parameters that will be explained further highlighted in red.

The gearbox is modelled with a ratio g whose value should be optimally designed and an efficiency λ. The gearbox torque referred to the low speed side, T_{gb}, for a gear ratio g in generating mode is given by:

$$T_{gb} = \frac{1}{\lambda}(gT_{gen} + [J_{gb} + g^2 J_{gen}]\frac{d\omega_\eta}{dt}) \tag{7}$$

where T_{gen} is the PMSG torque, J_{gb} and J_{gen} are inertia of the gearbox and the PMSG, λ is the gearbox efficiency and ω_η is the rotational velocity of the WEC's hinges.

In operational sea states, T_{gb} is dominated by the torque from the PMSG T_{gen} so this can be approximated by:

$$T_{gb} \approx \frac{1}{\lambda} g T_{gen} \tag{8}$$

The cost related maximum allowed torque of the gearbox, T^*_{gb}, is dependent on λ, g and the maximum output torque from the PMSG denoted as T^*_{gen} as:

$$T^*_{gb} \approx \frac{1}{\lambda} g T^*_{gen} \tag{9}$$

which pinpoints how the two optimisation variables g and T^*_{gen} influence the cost of the gearbox, and thus the LCoE.

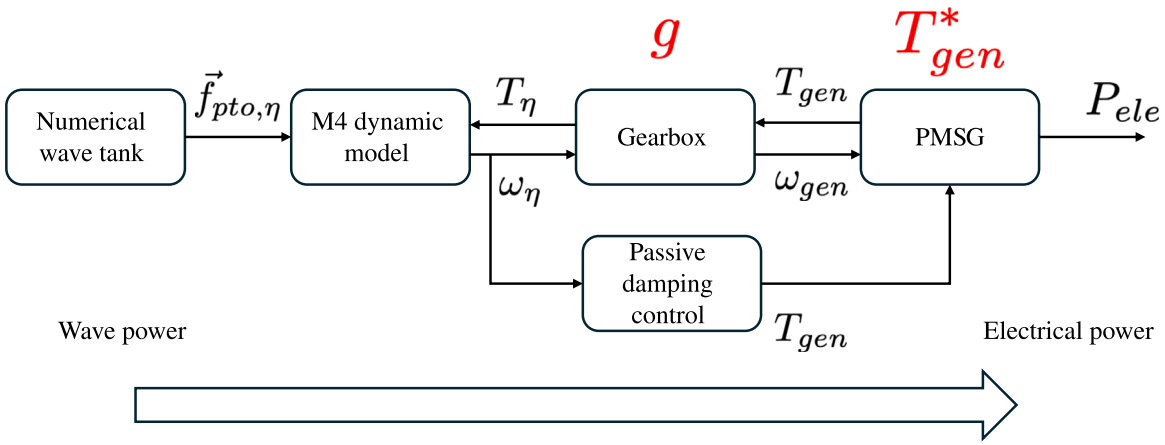

Fig. 2. Schematic diagram of the simplified PTO model used for co-design.

The gearbox efficiency λ is stage number (gear ratio) dependent, and generally lower for more stages. This is assumed here as [23,24]:

$$\lambda = \begin{cases} 0.98 & g \in (0,5] \\ 0.98^2 = 0.96 & g \in (5,25] \\ 0.98^3 = 0.94 & g \in (25,125] \\ 0.98^3 \times 0.97 = 0.91 & g \in (125,750] \\ 0.98^3 \times 0.97 \times 0.96 = 0.87 & g \in (750,4500] \end{cases}$$

Note that for simplicity the efficiency at rated power is used. In practice, this would vary as a function of operating point.

For the sake of computational efficiency of the co-design, the PMSG and its associated power electronic models are not simulated for either the line search method or the GA. Instead, the resultant torque–speed constraints from the drive train are considered for the upper-level WEC hydrodynamic simulations. Moreover, a PMSG design routine is proposed to estimate cost of the drive train and output parameters of the PMSG associated with the change of T^*_{gen}, including the winding resistance R_s, magnet flux ψ_m and core loss coefficients. Power losses of the drive train are then estimated using a post-processing function with these parameters, which will be introduced in the next section.

The PMSG power capacity, P^*_{gen}, is assumed fixed. In this work we let $P^*_{gen} = 12\,\text{kW}$. This is because the WEC's mean power capacity is slightly over 1 kW and with passive damping control the peak to mean power ratio is around 10. In fact, P^*_{gen} can be made an additional design parameter of the PTO which leads to a more complicated co-design problem.

For any value of the design parameter T^*_{gen}, there is a matching speed limit

$$\omega^*_{gen} = \frac{P^*_{gen}}{T^*_{gen}} \tag{10}$$

The torque and speed limit of the PMSG, together with the gearbox's ratio g decide the WEC's operational torque constraint T^*_η and speed constraint ω^*_η.

$$|T_\eta| \le T^*_\eta = gT^*_{gen} \tag{11}$$

and

$$|\omega_\eta| \le \omega^*_\eta = \frac{\omega^*_{gen}}{g} \tag{12}$$

In simulations, when the WEC hinge's rotational speed ω_η exceeds ω^*_η, the WEC will not receive any torque from the PMSG and so the PTO generates no power.

Mechanical power generation of the WEC under various sea wave conditions is influenced by these torque–speed constraints of the WEC, and thus the LCoE. In the next section, the LCoE performance function will be defined.

3. Definition of the simplified LCoE

The optimisation objective is to minimise the LCoE, which is taken as a performance function for the line search and a fitness function for the GA. The LCoE is defined as the total cost of the WEC system, including capital cost $CapEx$ and operational cost $OpEx$, over the generated electricity across an assumed 20-year lifetime.

$$LCoE = \frac{CapEx + OpEx}{E_{elc}} \tag{13}$$

The capital cost is the sum of the cost of the WEC mechanical platform and the cost of the PTO,

$$CapEx = C_{WEC} + C_{PTO} \tag{14}$$

Here we assume C_{PTO} is a fixed percentage of $CapEx$ [18,25],

$$C_{PTO} = 30\%CapEx \tag{15}$$

and the operational cost the same as the capital cost,

$$OpEx = CapEx \tag{16}$$

The electricity, in kWh, generated over the 20-year lifetime is calculated as

$$E_{elc} = \bar{P}_{site,elc}/1000 \times 175200\ \text{kWh} \tag{17}$$

where $\bar{P}_{site,elc}$ is the mean generated electrical power of the WEC system for a realistic sea site with varying sea states, with unit W. We use a new notation LCoE* to represent this simplified LCoE definition. The LCoE (13) can now be rewritten as

$$LCoE^* = \frac{\alpha C_{PTO}}{\bar{P}_{site,elc}} \tag{18}$$

where $\alpha = 0.038\ \text{h}^{-1}$ and the unit for the LCoE* is £/kWh.

3.1. Estimation of C_{PTO}

The cost of the PTO can be divided into three parts, representing the cost of three main components, the mechanical gearbox C_{gb}, the PMSG C_{gen} and C_{inv} representing the cost of power electronic components such as the AC/DC and DC/AC converters.

$$C_{PTO} = C_{gb} + C_{gen} + C_{inv} \tag{19}$$

3.1.1. Cost of the gearbox

For mechanical gearboxes, costs are scaled with maximum torque T^*_{gb} at low speed side. For a 3-stage planetary gearbox, with gear ratios $25 \le g \le 125$, an estimation of this is [23,24,26]:

$$C_{gb} = T^*_{gb} \times 0.18\,£/\text{N m} \tag{20}$$

For more stages, i.e. higher gear ratios, penalties can be added. Here we assume a 10% increase of C_{gb} for each additional stage and 10% decrease for each less based on (20).

$$C_{gb} = \begin{cases} T^*_{gb} \times 0.146\,£/\mathrm{N\,m} & g \in (0,5] \\ T^*_{gb} \times 0.162\,£/\mathrm{N\,m} & g \in (5,25] \\ T^*_{gb} \times 0.180\,£/\mathrm{N\,m} & g \in (25,125] \\ T^*_{gb} \times 0.198\,£/\mathrm{N\,m} & g \in (125,750] \\ T^*_{gb} \times 0.218\,£/\mathrm{N\,m} & g \in (750,4500] \end{cases}$$

3.1.2. Cost of the PMSG and converters

A design routine for the electric drive is used to estimate the cost of the PMSG and converters. The design routine takes torque T^*_{gen}, speed ω^*_{gen}, and pole-number (which is fixed at 8 for this work) as input variables and adopts classic sizing equations [27] based on sensible electric and magnetic loading values for forced air cooled PMSGs [28] (see Appendix B for the key design parameters). The routine returns the amount of copper, PM, lamination and structural steel materials for the PMSG, and the values of losses and the main electric parameters. The PMSG cost is given by

$$C_{gen} = M_{Cu}C_{Cu}f_{slot}(N_s) + M_{PM}C_{PM} + M_{core}C_{core} + M_{str}C_{str} \tag{21}$$

where copper, PM, lamination and structural masses $\{M_{Cu}, M_{PM}, M_{core}, M_{str}\}$ are estimated by the PMSG design routine and unit prices $\{C_{Cu}, C_{PM}, C_{core}, C_{str}\}$ are given in Appendix A along with function $f_{slot}(N_s)$ accounting for labour increase with the number of slots N_s.

The rated power and power factor provide the kVA ratings for the converter which allow estimating the cost based on the correlation proposed in [7], here adjusted for inflation to the year of 2024. The cost of converters is then estimated as [7]

$$C_{inv} = 7.973 \times (PF_{gen}P^*_{gen})^{0.7} \tag{22}$$

where P^*_{gen} is the PMSG rated (design) power, PF_{gen} is the PMSG rated power factor estimated by the design routine.

3.2. Estimation of $\bar{P}_{site,elc}$

The mean electrical power is estimated by numerical simulations using the state-space WEC hydrodynamic model. For the M4 WEC considered, realistic sea states from the sea trial site at King George Sound, Albany, Western Australia are used to generate input wave profiles. Fig. 3 shows a scatter diagram of relevant wave conditions measured at King George Sound, Albany, Western Australia in summer (Nov–March), where the ocean test of the M4 WEC will take place. Sea states with significant wave height (H_s) from 0.5 m to 1.5 m and peak periods (T_p) from 3.5 s to 9.1 s are considered, which gives 45 sea states in total and cover wave conditions for 96% of the time. The remaining 4% are sea states with low occurrence rate, which are neglected here to reduce computational burden. Note that peak periods T_p are assumed to be 1.2 times the mean periods shown in the horizontal axis in Fig. 3. Table 1 summarises these sea states' occurrence as a percentage. The JONSWAP wave spectrum with a peak enhancement factor of $\gamma = 3.3$ is used to generate uni-directional irregular wave profiles of these conditions. For each sea state, the run time is $t_N = 600$ s for estimating the mean generated electrical power.

To reduce computational burden, numerical simulations are run on the WEC hydrodynamic model with torque–speed constraints instead of the integrated WEC-PTO model, as discussed. The variation of co-design parameters, the gearbox ratio g and the PMSG torque limit T^*_{gen} are translated into torque–speed constraints T^*_η and ω^*_η as presented in Section 2.2. This results in a rectangular-shaped constraint area of the WEC's torque and speed. Field-weakening mechanism that allows temporary over-speeding of the PMSG is omitted here, which leads to a slight underestimation of power generation in high sea states [7].

Table 1
Wave conditions and occurrence rate in percentage (%).

T_p (s)\H_s (m)	0.5	0.75	1	1.25	1.5
3.5	2.32	0.83	0	0	0
4.2	5.12	6.08	0.87	0	0
4.9	5.63	7.93	5.91	0.52	0
5.6	5.21	6.06	4.62	3.2	0.28
6.3	4.32	4.8	2.74	2.43	2.07
7	3.31	3.71	2.03	1.15	1.16
7.7	2.1	2.63	1.41	0.68	0.41
8.4	1	1.39	1.09	0.5	0.33
9.1	0.32	0.63	0.63	0.32	0.23

For each sea state, simulations output torque and angular velocity time profiles $T_\eta(t)$ and $\omega_\eta(t)$. Mean mechanical power can be calculated as:

$$\bar{P}_{i,mech} = \frac{\lambda \int_{t=0}^{t_N} -T_\eta \omega_\eta dt}{t_N} \tag{23}$$

Here, i is the index of the specific sea state and $i = 1, 2, \ldots, 45$. Note that gearbox efficiency λ is used as a multiplier here to factor in power loss of the gearbox so $\bar{P}_{i,mech}$ is the mechanical power received by the PMSG excluding gearbox loss.

Mean copper loss can be calculated from torque-producing current profile as:

$$\bar{P}_{i,Cu} = \frac{R_s \int_{t=0}^{t_N} i_q^2 dt}{t_N} \tag{24}$$

where R_s is the winding resistance. The torque producing current profile neglecting field-weakening effect is

$$i_q = \frac{T_\eta}{gp\psi_m} \tag{25}$$

where p is the number of pole pairs and ψ_m is the magnet flux of the PMSG as discussed. Both R_s and ψ_m are outputs of the drive train design routine.

Classic core loss calculation methods used in PMSGs refer to steady-state constant frequency operation while in WECs the rotor undergoes an oscillatory movement. To get a rough estimate of core losses in such a scenario, the oscillatory generator speed was treated as a slowly-varying fundamental frequency (scaled with p) feeding in the Bertotti formulation. The design routine also outputs coefficients $\{k_{hy}, k_{ed}, k_{ex}\}$ of Bertotti core-loss formulation rewritten in global terms as a function of the mechanical speed

$$P_{Fe} = k_{hy}|\omega_{gen}| + k_{ed}|\omega_{gen}|^2 + k_{ex}|\omega_{gen}|^{1.5} \tag{26}$$

which gives 'instantaneous' core loss P_{Fe}. The mean core loss for sea state i can then be calculated as

$$\bar{P}_{i,Fe} = \frac{\int_{t=0}^{t_N} P_{Fe} dt}{t_N} \tag{27}$$

The mean electrical power for sea state i can be calculated by subtracting mean copper and core loss from the mean mechanical power

$$\bar{P}_{i,elc} = \bar{P}_{i,mech} - \bar{P}_{i,Cu} - \bar{P}_{i,Fe} \tag{28}$$

where inverters loss is neglected.

Mean electrical power for the site can be calculated as a weighted sum using the occurrence rate of each sea state ξ_i shown in Table 1 as:

$$\bar{P}_{site,elc} = \sum_{i=1}^{45} \frac{\bar{P}_{i,elc}\xi_i}{96\%} \tag{29}$$

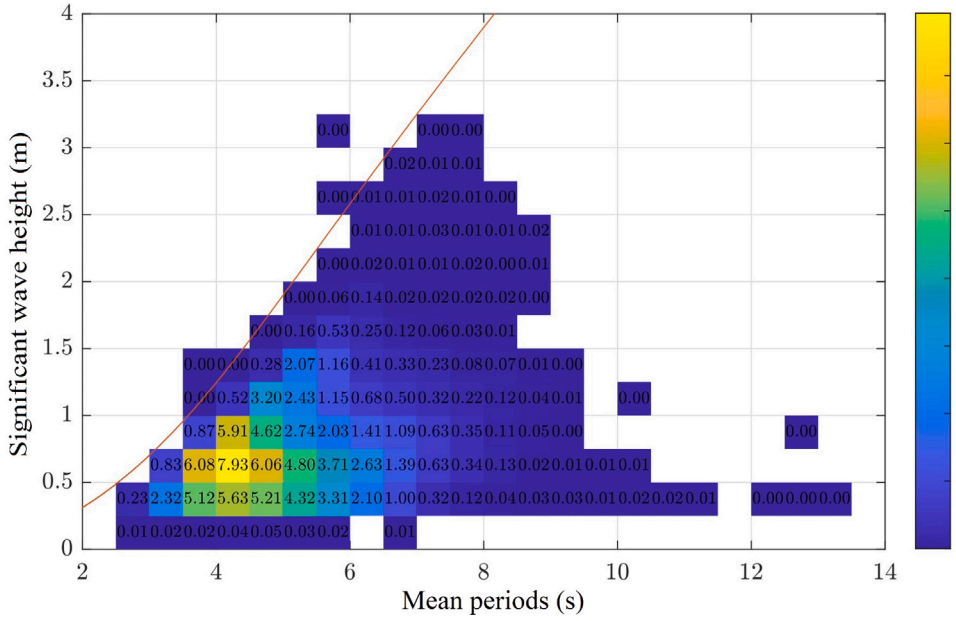

Fig. 3. Scatter diagram [12] of the wave climate at the considered site. Each block represents a specific sea state in which its occurrence rate is shown as a percentage.

4. Problem definition and optimisation algorithms

The co-design objective is to search for an optimal set of design parameters (in this case the gearbox ratio g and PMSG torque limit T^*_{gen} pair) that minimises the performance index LCoE* shown as (18). In this section, two search algorithms are proposed. The first one is the traditional line search algorithm which involves high computational efforts, serving as a benchmark. The second one is a GA, which has a potential of reducing the co-design efforts dramatically.

4.1. The line search approach

For the line search approach, sensible ranges of the design parameters g and T^*_{gen} need to be defined. In [16], a pair of parameters $g = 739$ and $T^*_{gen} = 50\,\mathrm{N\,m}$ are used for the M4 drive train, which provides a starting point for selecting the ranges. In this paper, the gearbox ratio is varied from $g = 100$ to $g = 1200$, with a step size of 100, while the PMSG torque limit is set to vary from $T^*_{gen} = 10\,\mathrm{N\,m}$ to $T^*_{gen} = 120\,\mathrm{N\,m}$, with a step size of $10\,\mathrm{N\,m}$. A finer step size provides more accurate design results but can lead to higher computational burden when performing the line search.

Fig. 4(a) shows the design flowchart of the line search method. Two iteration loops, with indexes i and j, are required to traverse ranges of the two design parameters. At each iterative step, g_i and $T^*_{gen,j}$ are converted to torque and speed limits T^*_η and ω^*_η, passed on to the WEC simulation function. Meanwhile, g_i and $T^*_{gen,j}$ are sent to the drive train design routine for the calculation of C_{pto}, as well as R_s, ψ_m and $\{k_{hy}, k_{ed}, k_{ex}\}$ for estimating the PMSG loss. A post-processing function is then used to merge these results and output the $\mathrm{LCoE}^*_{i,j}$ for the specific pair of parameters g_i and $T^*_{gen,j}$. In the end, the algorithm outputs the best pair of g and T^*_{gen} that gives minimum LCoE*.

4.2. The genetic algorithm

The GA takes a different way to search the optimal set of design parameters. A flowchart of the GA's procedure is shown in Fig. 4(b). Instead of iterating through each combination of the design parameters in range, the algorithm generates a specified number, N_i, sets of parameters to form the first generation of population. Each set of parameter, g and T^*_{gen}, is called an individual. The fitness function LCoE* for each individual is then estimated using the same simulation, drive train design routine and post-processing function as for the line search method. These individuals are then sorted by their scores from high to low (in this case, a low LCoE* means a high score). Individuals with higher scores have a higher chance to be selected as parents to breed the next generation.

There are three different operations when it comes to breeding the offspring, namely replication, crossover and mutation. Replication means the parent, usually with the highest score, is maintained in the next generation. This allows the GA to preserve the best searching result as the population evolves. Crossover takes two parents, swaps some of their genes (design parameters) to generate offspring. This can potentially produce higher score children as the high quality genes are inherited by them. Mutation takes one parent, and randomly varies some of its genes to generate an offspring. In practice, this allows the algorithm to explore the searching space, hopefully jumping out of a local optimum for a global optimum. The percentages of crossover and mutation operations, ξ_{cr} and ξ_{mu} are tuning parameters of the GA.

For each succeeding generation, the same scoring, parent selection and breeding processes are done, until the maximum number of generations N_g is reached. It can be noticed immediately that the computational burden of the GA is dependent on the number of generation N_g and population size within each generation N_i and independent of the number of design parameters. The results of applying the GA to the PTO co-design problem will be demonstrated in the next section, in comparison to the line search method.

5. Results

In this section, the co-design results are presented for both the line search and the GA. These are run with Matlab_R2023b on a MacBook Pro device with the Apple M3 chip. Sampling rate of the WEC state-space model is $0.1\,\mathrm{s}$.

5.1. Line search results

Results given by the line search method are presented here as a benchmark to the GA shown in Figs. 5 to 8. Contours are plotted to provide better observation of these results. Fig. 5(a) shows that C_{gb} scales with both g and T^*_{gen}, as T^*_{gb} depends on both. Fig. 5(b) and (c)

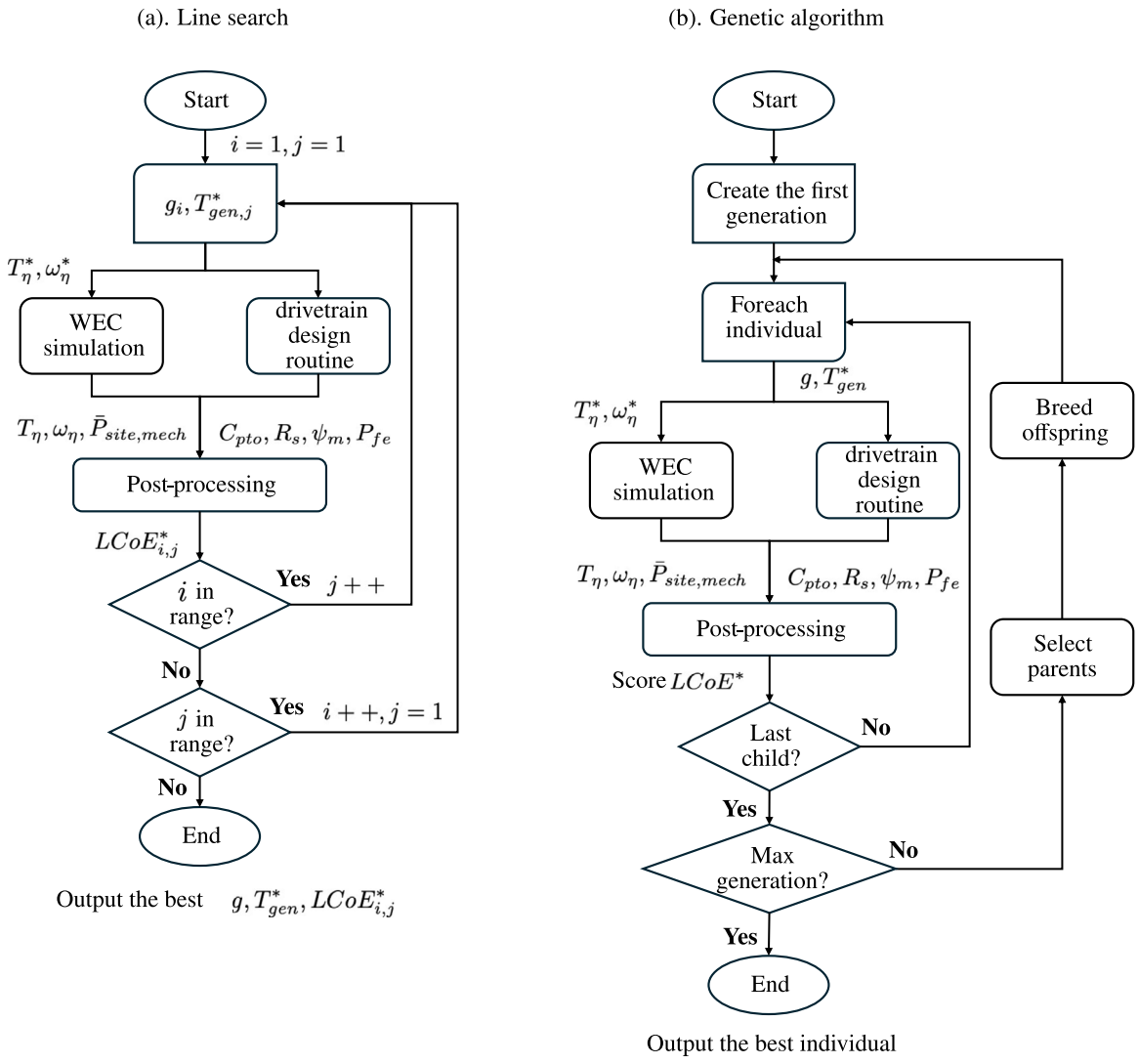

Fig. 4. Co-design flowchart using (a) the iterative line search approach and (b) the genetic algorithm.

show that C_{gen} and C_{inv} are independent of g as expected. But C_{gen} increases as T^*_{gen} increases while C_{inv} is high for low T^*_{gen}. This can be attributed to the rise of power factor at higher speed (low T^*_{gen}) due to increased reactance, which means higher kVA demand for the converters and then cost. However, the range of C_{inv} is noticeably small, because the rated power P^*_{gen} is fixed. The cost of the PTO in total, C_{pto}, is the sum of Fig. 5(a), (b) and (c), as shown in Fig. 5(d). Generally, C_{pto} is high for bigger values of g and T^*_{gen}. At this scale of the PTO, the gearbox cost contributes the most to C_{pto}.

Mean electrical power for all combinations of g and T^*_{gen} is shown in Fig. 6. The red point indicates the optimum electrical power. The highest value of $\bar{P}_{site,elc} = 1280.99\,\text{W}$, is obtained with $g = 700$ and $T^*_{gen} = 60\,\text{N m}$. Fig. 7 gives gearbox loss, copper and core loss estimation to help with the observation of Fig. 6. It can be noticed that, sub-optimal designs of T^*_{gen} and g generally lead to higher PTO losses, which impacts electricity generation negatively.

Fig. 8 shows the line search result for optimum LCoE*. A white area in the left-bottom corner of searching surface can be noticed, with $g = 100$ and $T^*_{gen} = 10\,\text{N m}, 20\,\text{N m}, 30\,\text{N m}$. There is near zero or negative electricity generation with these choices of parameters so the LCoE* is ill-defined. The red point in the plot indicates the minimum. The minimum LCoE* is $0.2792\,£/\text{kWh}$, obtained with $g = 700$ and $T^*_{gen} = 30\,\text{N m}$. Comments can be made here by comparing the line search results with the actual M4 system tested in Albany [16]. Results here show that the optimal gear ratio is 700:1 while the actual Albany system has a gearbox ratio of 739:1. Optimal T^*_{gen} is between $60\,\text{N m}$ and $30\,\text{N m}$ depending on which objective is considered, maximum power or minimum LCoE*, while the Albany system uses two generators with combined T^*_{gen} around $50\,\text{N m}$. These validate that the PTO co-design problem here is practical and results are informative for actual system design.

In Fig. 8, the LCoE* ranges from a minimum value of $0.2792\,£/\text{kWh}$ to $9.9798\,£/\text{kWh}$ at the right-top corner, which suggests the optimum co-design of the PTO parameters is essential for LCoE reduction of WECs. It should be also pointed out that the optimal design for maximum power does not necessarily give minimum LCoE*, which can be found by comparing the optimum points in Figs. 6 and 8. In fact, the LCoE* for maximum power is $0.3812\,£/\text{kWh}$. This means when it comes to optimum WEC co-design, using only power generation as a performance function can be misleading. However, using LCoE as an objective function requires a model to estimate the cost of the WEC, which is not an easy task. Here we use a simplified cost model to demonstrate the PTO co-design problem.

5.2. Genetic algorithm results

The GA is applied to resolve this PTO co-design problem by using the Matlab GA routine 'ga'. Here we let the maximum generation $N_g =$

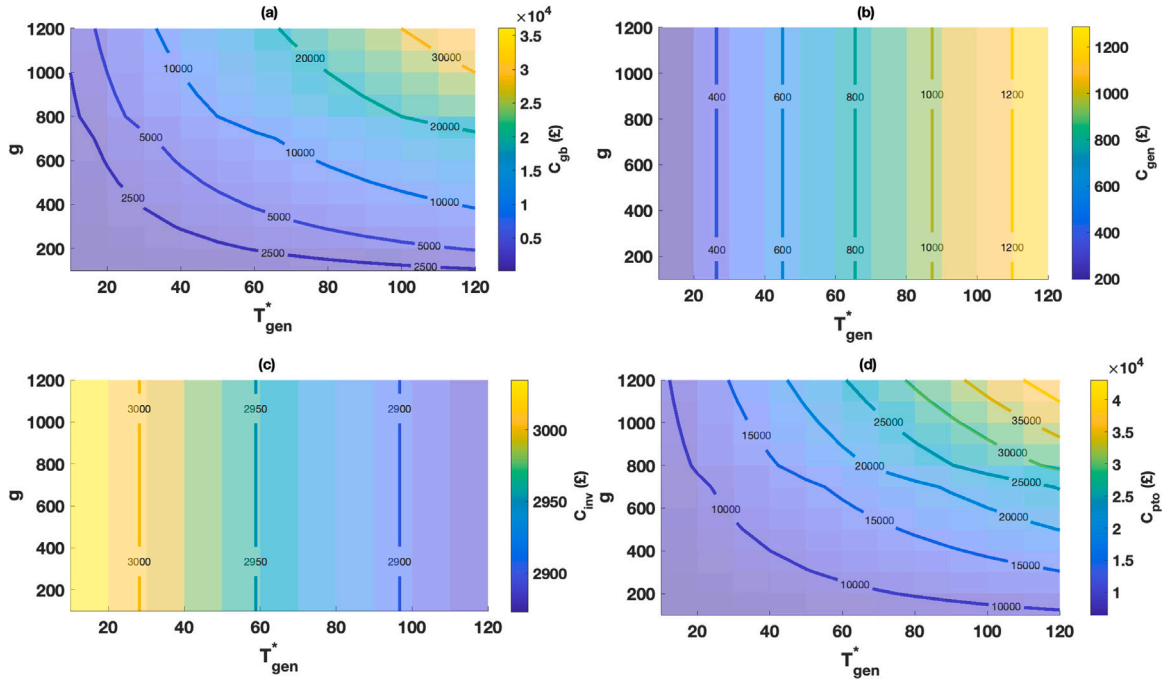

Fig. 5. Cost estimation of the PTO components and total: (a) gearbox cost, (b) PMSG cost, (c) converters cost, (d) PTO cost.

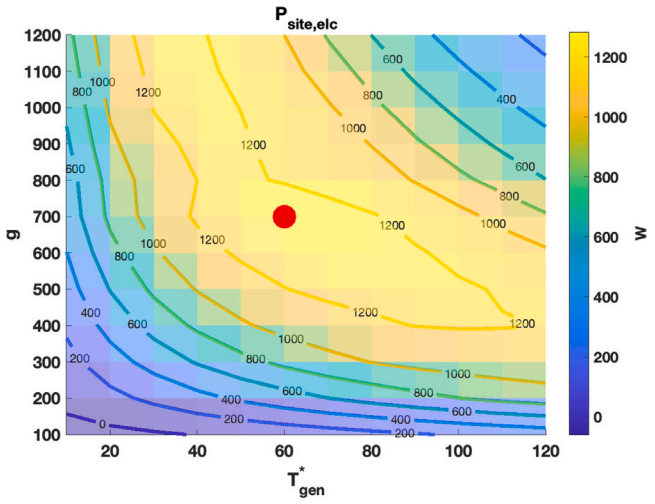

Fig. 6. Weighted electrical power of the considered site. The red point represents maximum electrical power.

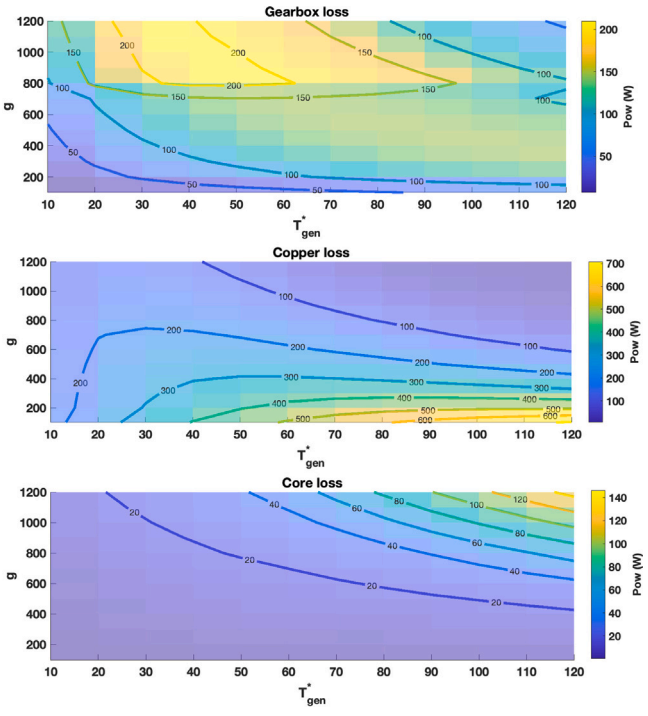

Fig. 7. Gearbox loss, copper and core loss estimation for the considered site.

5 and population size $N_i = 10$. The crossover and mutation rate are $\xi_{cr} = 0.8$ and $\xi_{mu} = 0.2$, respectively. For the first generation, the four corner points $T^*_{gen} = 10\,\mathrm{N\,m}, g = 100$, $T^*_{gen} = 10\,\mathrm{N\,m}, g = 1200$, $T^*_{gen} = 120\,\mathrm{N\,m}, g = 100$, $T^*_{gen} = 120\,\mathrm{N\,m}, g = 1200$ are included intentionally. The other six individuals are selected so that they distributed evenly in the search ranges of T^*_{gen} and g, with $T^*_{gen} = 40, 90\,\mathrm{N\,m}$ and $g = 300, 650, 1000$. Note that design parameters T^*_{gen} and g are assumed to be integer values when applying the GA.

Table 2 summarises the evolution of the population as well as the score for each individual, over the five generations. Individuals are sorted by their LCoE* from low to high so individual 1 represents the best in its generation. It can be noticed that the mean LCoE* decreases dramatically from the first to the second generation, and keeps decreasing over the five generations. This suggests the GA enables evolution of the initial population towards the direction of a low value of LCoE*.

It can be also noticed from Table 2 that new elites emerge for the first two generations of offspring. In the second generation, the best individual has an LCoE* of 0.2895 £/kWh with $T^*_{gen} = 31\,\mathrm{N\,m}$ and g = 569. In the third generation, the best individual has an LCoE* equals 0.2784 £/kWh with $T^*_{gen} = 28\,\mathrm{N\,m}$ and g = 699, slightly surpassing the optimum LCoE* of 0.2792 £/kWh suggested by the line search method. Comparing the values of T^*_{gen} and g, for line search $T^*_{gen} = 30\,\mathrm{N\,m}$, g = 700 and for the GA $T^*_{gen} = 28\,\mathrm{N\,m}$, g = 699, it is understood that this elite represents an optimum point missed by the line search

Table 2
Evolution of the population using GA to solve the co-design problem, $N_i = 10$ and $N_g = 5$. The symbol 'NaN' represents an ill-defined point of the LCoE* due to zero or negative electricity generation.

Generation	1st			2nd			3rd			4th			5th		
Individuals	Tgen*	g	LCoE*	Tgen*	g	LCoE*	Tgen*	g	LCoE*	Tgen*	g	LCoE*	Tgen*	g	LCoE*
1	40	650	**0.2948**	31	569	**0.2895**	28	699	**0.2784**	28	699	**0.2784**	28	699	**0.2784**
2	10	1200	**0.3189**	40	650	**0.2948**	31	569	**0.2895**	32	721	**0.282**	30	697	**0.2793**
3	90	300	**0.3528**	10	1200	**0.3189**	40	650	**0.2948**	31	569	**0.2895**	32	697	**0.2817**
4	40	300	**0.3784**	40	348	**0.3417**	40	413	**0.3136**	38	697	**0.2938**	32	721	**0.282**
5	40	1000	**0.4175**	90	312	**0.3532**	37	388	**0.3278**	38	430	**0.3109**	30	623	**0.2839**
6	90	650	**0.5334**	40	824	**0.3703**	63	323	**0.3309**	39	417	**0.3136**	38	419	**0.3142**
7	120	100	**0.8425**	65	650	**0.387**	38	375	**0.3317**	38	380	**0.3294**	37	421	**0.315**
8	90	1000	**1.4497**	100	201	**0.3973**	32	910	**0.3444**	33	390	**0.3373**	31	885	**0.3372**
9	120	1200	**9.9798**	101	420	**0.4154**	33	316	**0.3931**	24	335	**0.4391**	38	788	**0.3547**
10	10	100	**NaN**	10	100	**NaN**	93	925	**1.2872**	65	901	**0.6171**	67	914	**0.6512**
Mean			**1.6186**			**0.3520**			**0.4191**			**0.3491**			**0.3378**

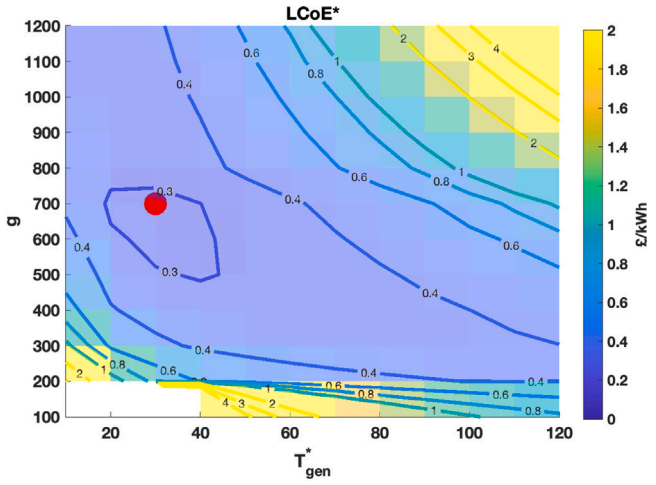

Fig. 8. LCoE* of the considered site. The red point represents minimum LCoE*.

due to the selection of a sparse searching step. Although these two optimum points suggested both methods can be deemed the same for this specific co-design problem, the GA can potentially outperform the line search if the searching ranges are not properly selected for the latter.

This elite from the third generation remains the best over all five generations, which indicates the GA converges to an optimum point only after two generations for this problem. This is achieved by carefully tuning the crossover and mutation ratios ξ_{cr} and ξ_{mu} as well as selecting the initial population that spans the searching range as evenly as possible. The parameters ξ_{cr}, ξ_{mu}, N_i and N_g are essential to the effectiveness of the GA and the tuning of them are highly problem dependent. A detailed discussion on how to tune these parameters is out of the scope of this paper as the main focus is to demonstrate the GA's effectiveness in resolving WEC co-design problems.

Fig. 9 presents a visualisation of Table 2, by plotting each individual's position on the LCoE* line search surface, where contours are generated from the line search results as for Fig. 8. Populations are grouped by their generation with different markers. The red filled circle and triangle represent the optimum design point given by the line search method and the GA, respectively. Initial population is represented by marker '+' and one can see how these individuals are evenly distributed in the searching space. It can also be noticed that as the population evolves, successive individuals are grouping more closely to low LCoE* areas, demonstrating again the effectiveness of the GA.

5.3. Comparison of computational burden

A key performance index for co-design methods is their computational burden. In this subsection we compare the computational time needed for both the line search method and the GA.

The WEC hydrodynamic model simulation is the most time consuming part of the searching. With state-space model introduced in Section 2, a simulation with 600 s' wave profile in Matlab takes approximately 4 s. To estimate $\bar{P}_{site,mech}$, 45 sea states need to be run, which cost 180 s in total for any set of design parameter candidate. This is called a site simulation here.

In our co-design problem, there are only two design parameters, T^*_{gen} and g. For the line search method, 12 values are defined in each of their ranges, resulting in 144 pairs of T^*_{gen} and g to be tested, and thus 144 site simulations have to be run. In total, this takes approximately 25 920 s, or 7.2 h. For the GA, there are 10 individuals in each generation and the maximum number of generation N_g is set to 5 which is more than enough to ensure convergence. This leads to 50 individuals to be tested, thus 50 site simulations, which takes only 9000 s or 2.5 h, approximately 1/3 of what the line search needs.

The advantage of using the GA gets more obvious as the number of design parameters increases. An estimation of this is shown in Fig. 10. Here we assume for the line search, 12 values are defined in the range for each additional design parameter. The number of site simulations needed rises dramatically as the number of design parameters increases. With 4 design parameters, the line search method can take more than 1000 h, which is unacceptably time demanding. Clearly, the line search method is too time consuming and unmanageable with a high number of design parameters. Although this can be potentially reduced by narrowing down the searching range or running simulations in parallel, it inevitably makes the co-design method more difficult to automate. On the other hand, the computational burden for the GA is less dependent of the number of design parameters. Here we assume for each additional design parameter, the maximum generation N_g is doubled to reach an optimum. Also, the population size N_i is assumed to increase from 10 for two design parameters here, to 30 for three and 90 for four, respectively. Even so, the time required for a 4-parameter co-design problem is less than 10 h.

When addressing co-design problems involving a significant number of design parameters, it is evident that the line search method is less efficient. In contrast, the GA emerges as a highly effective and efficient tool for tackling such complex tasks.

5.4. Estimation of LCoE* reduction with up-scaling of the M4 capacity

LCoE reduction is essential for wave energy. In this section, we demonstrate that this can also achieved by up-scaling of the WEC capacity and provide an estimation of the LCoE* of the M4 WEC at different scales. This is done by up-scaling the mean electrical power $\bar{P}_{site,elc}$ based on Froude scaling. Assuming the current 20 m long WEC as unit scale and denote the scaling factor as s, mean electrical power can be scaled as

$$\bar{P}_{site,elc,s} = \bar{P}_{site,elc} s^{3.5} \tag{30}$$

and torque and speed can be scaled accordingly with ratio s^4 and $s^{-0.5}$, respectively. Realistic sea waves are directional, which is not considered in the co-design simulation. Here we assume a 20% reduction of power generation with spreading waves, and a multiplier of 0.8

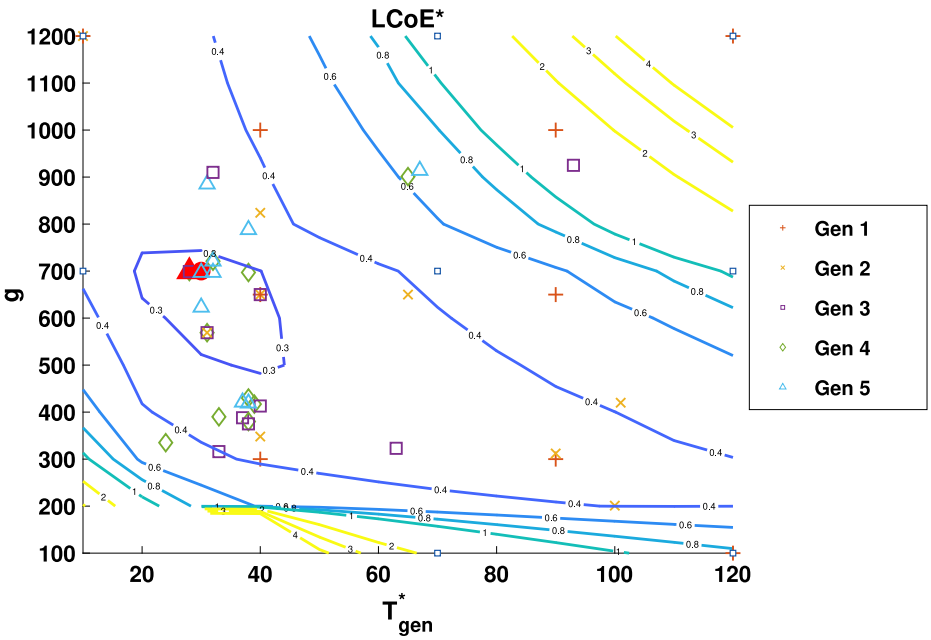

Fig. 9. Co-design results of the LCoE* with the GA. Individuals of the same generation are represented by the same markers. The red filled circle represents optimum point of the line search results while the red filled triangle represents the elite of the GA.

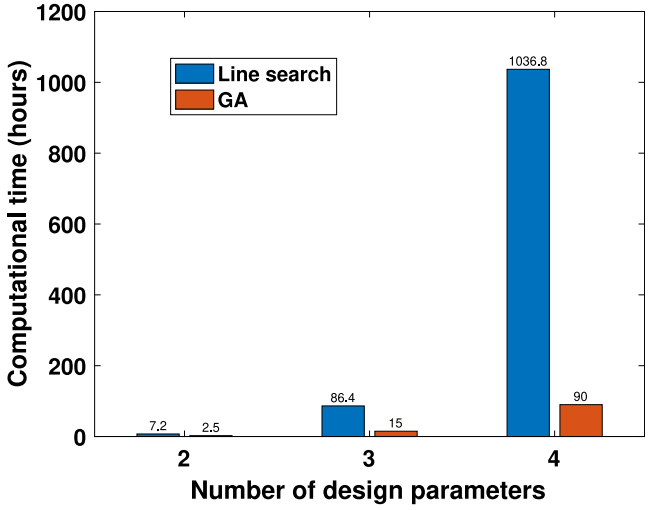

Fig. 10. Estimation of computational time needed for the line search method and the GA, with different numbers of design parameters.

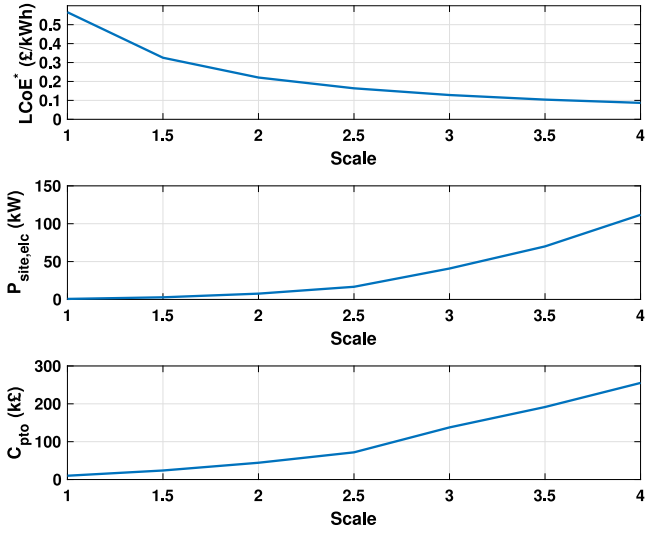

Fig. 11. Estimation of LCoE* reduction by up-scaling of the WEC capacity. Top: LCoE*, middle: mean electrical power, bottom: cost of the PTO.

is applied to $\bar{P}_{site,elc,s}$. This is based on power reduction analysis on different M4 configurations under directional wave conditions [29,30]. This should also include the up-scaling of the PMSG rated power P^*_{gen} and rated torque T^*_{gen}. Note that the optimum design parameters, T^*_{gen} and g, will certainly change for different scales of the WEC, but this is not the main concern here. The PTO cost is re-accessed using the drive train design routine. Also note that the cost of energy storage component is neglected when solving the co-design problem. Here we use supercapacitor for power smoothing and it is estimated that this costs 20% more than the gearbox based on Albany experience, which is added to re-calculate the LCoE* when performing the up-scaling.

Fig. 11 shows the estimation of optimum LCoE*, corresponding mean electrical power and PTO cost from top to bottom. It can be observed that with the increase of WEC scale, optimum LCoE* decreases, from 0.57 £/kWh with $s = 1$, to 0.22 £/kWh with $s = 2$ and 0.09 £/kWh with $s = 4$. With $s = 4$ the WEC is approximately 80 m long with mean electrical power of 112 kW. A MW generator will be required. At this capacity, LCoE* of wave energy becomes commercially competitive. Note that we limit the analysis of LCoE up to 1-MW capacity. For higher capacity, the availability of PTO technology is currently unknown. Although this is a rough estimation based on a simplified version of the LCoE, it demonstrates an LCoE reduction pathway for wave energy by the up-scaling of WEC capacity.

6. Conclusions and future directions

A typical and realistic PTO co-design problem is addressed in this paper. The multi-float M4 WEC in development for a planned sea trial uses an electrical drive train as its PTO. The drive train's gearbox ratio and generator's rated torque are two key parameters to be optimised. WEC hydrodynamic simulations are run with 45 irregular sea states as

inputs to estimate mechanical power capture for the site. Note here unidirectional waves with $\gamma = 3.3$ are assumed in the absence of spreading and bandwidth information. The design parameters are modelled as torque–speed constraints for these simulations. A drive train design routine is proposed to estimate the cost of the drive train for different input design parameters. A simplified version of the LCoE is used as a performance function, evaluated in a post-processing manner to speed up the co-design procedure. A traditional iterative line search approach is applied to obtain optimum design as a benchmark. Line search results are consistent with the actual M4 PTO system tested in Albany, validating the co-design problem is practical. It is also found that using minimum LCoE or maximum power as objective functions yields different design solutions.

The genetic algorithm is applied to resolve this PTO co-design problem for the first time. It is found that the GA effectively converges to an optimum design point and the main advantage is in its requirement of less computational efforts, approximately 1/3 the time needed for line search. The GA will be more efficient for more complicated WEC co-design problems with a higher number of design parameters. The main challenge of using the GA algorithm to resolve the WEC co-design problem is in the design of the first generation, to cover as many 'genetic possibilities' as possible.

LCoE reduction is essential for WECs. In this paper, it is demonstrated this can be achieved at two levels. Firstly, optimum co-design of PTO parameters contributes to the LCoE reduction profoundly. It is also found that optimum design that gives maximum power does not necessarily give minimum LCoE. Secondly, the up-scaling of WEC capacity also enables LCoE reduction. An estimation of LCoE* at different capacities is given. This is done by up-scaling the mean electrical power with Froude scaling and accounting for directional waves with a power reduction multiplier. PTO cost is re-accessed at different scales using the proposed drive train design routine and including energy storage component. The estimation is LCoE* is reduced by a factor of 6 from 10-kW capacity to 1-MW capacity of the M4 WEC.

A simple passive damping controller with a well-tuned damping ratio is assumed for the WEC system in this work. In due course, this should be extended to include more advanced energy-maximising controllers, which leads to more sophisticated control co-design problems. The optimum PTO parameters will be different when different control strategies are applied. This also requires more detailed control formulations including handling shut-down conditions in extreme sea states. Controller tuning parameters have to be incorporated as extra co-design parameters which will increase the dimension and complexity of the current co-design problem. The proposed co-design framework is applicable for these CCD problems thanks to the decoupling of WEC simulation and PTO loss and cost estimations. Besides, the advantages of using the GA-based approach will become more obvious due to its computational efficiency.

CRediT authorship contribution statement

Zhijing Liao: Writing – original draft, Visualization, Validation, Investigation, Formal analysis. **Guang Li:** Writing – review & editing, Supervision, Conceptualization. **Judith Apsley:** Writing – review & editing, Supervision, Methodology, Investigation. **Matteo F. Iacchetti:** Writing – review & editing, Validation, Methodology. **Peter Stansby:** Writing – review & editing, Validation.

Declaration of competing interest

The authors declare that they have no known competing financial interests or personal relationships that could have appeared to influence the work reported in this paper.

Acknowledgements

The authors would like to acknowledge the funding from the Engineering and Physical Sciences Research Council (EPSRC), United Kingdom with grant number EPV0405101, and a funding from National Natural Science Foundation of China (NSFC) with grant no. 62473180. The M4 WEC was designed in the Blue Economy CRC Project Plan P.3.21.004: Seeding marine innovation in SW WA with a WEC deployment in Albany, funded by the Government of Western Australia, Australia, Blue-Economy Cooperative Research Centre, and The University of Western Australia, Australia. Fig. 1 is kindly provided by BMT, Australia.

Appendix A

Unit prices (including labour) and correction for slot number are presented below. These were calibrated to match the price of a few benchmark PMSGs found online.

$$C_{Cu} = 70\,£/\mathrm{kg} \tag{A.1}$$

$$C_{PM} = 172\,£/\mathrm{kg} \tag{A.2}$$

$$C_{core} = 6\,£/\mathrm{kg} \tag{A.3}$$

$$C_{str} = 8\,£/\mathrm{kg} \tag{A.4}$$

$$f_{slot}(N_s) = 3\left(\frac{N_s}{18} - 1\right) \tag{A.5}$$

Appendix B

PMSM design parameters are presented below based on standard practice for air-cooled PM machines. Electric loading: $A_{rms} = 40\,\mathrm{kA/m}$; current density: $J_{rms} = 6\,\mathrm{A/mm^2}$; magnetic loading: $B_{g1} = 0.8$ T; PM-to-pole arc ratio: $\alpha_{PM} = 0.8$. N33H PM grade operating at 120 °C. Yoke and tooth prescribed flux–density are 1.2 T and 1.8 T.

References

[1] K. Gunn, C. Stock-Williams, Quantifying the global wave power resource, Renew. Energy 44 (2012) 296–304, http://dx.doi.org/10.1016/j.renene.2012.01.101, URL http://www.sciencedirect.com/science/article/pii/S0960148112001310.

[2] R.A. Arinaga, K.F. Cheung, Atlas of global wave energy from 10 years of reanalysis and hindcast data, Renew. Energy 39 (1) (2012) 49–64, http://dx.doi.org/10.1016/j.renene.2011.06.039, URL https://www.sciencedirect.com/science/article/pii/S0960148111003764.

[3] M. Penalba, J.V. Ringwood, A review of wave-to-wire models for wave energy converters, Energies 9 (7) (2016) http://dx.doi.org/10.3390/en9070506, URL https://www.mdpi.com/1996-1073/9/7/506.

[4] M. Garcia-Sanz, Control Co-Design: An engineering game changer, Adv. Control Appl. 1 (1) (2019) e18, http://dx.doi.org/10.1002/adc2.18, e18 ADC2-19-0039. arXiv:https://onlinelibrary.wiley.com/doi/pdf/10.1002/adc2.18. URL https://onlinelibrary.wiley.com/doi/abs/10.1002/adc2.18.

[5] M. Rosati, J.V. Ringwood, Control co-design of power take-off and bypass valve for OWC-based wave energy conversion systems, Renew. Energy 219 (2023) 119523, http://dx.doi.org/10.1016/j.renene.2023.119523, URL https://www.sciencedirect.com/science/article/pii/S0960148123014386.

[6] J. Grasberger, L. Yang, G. Bacelli, L. Zuo, Control co-design and optimization of oscillating-surge wave energy converter, Renew. Energy 225 (2024) 120234, http://dx.doi.org/10.1016/j.renene.2024.120234, URL https://www.sciencedirect.com/science/article/pii/S0960148124002994.

[7] J. Aubry, H. Ben Ahmed, B. Multon, Sizing optimization methodology of a surface permanent magnet machine-converter system over a torque-speed operating profile: Application to a wave energy converter, IEEE Trans. Ind. Electron. 59 (5) (2012) 2116–2125, http://dx.doi.org/10.1109/TIE.2011.2163287.

[8] C.A.M. Ströfer, D.T. Gaebele, R.G. Coe, G. Bacelli, Control co-design of power take-off systems for wave energy converters using WecOptTool, IEEE Trans. Sustain. Energy 14 (4) (2023) 2157–2167, http://dx.doi.org/10.1109/TSTE.2023.3272868.

[9] J.V. Ringwood, Control co-design for wave energy systems, Appl. Ocean Res. 158 (2025) 104514, http://dx.doi.org/10.1016/j.apor.2025.104514, URL https://www.sciencedirect.com/science/article/pii/S0141118725001026.

[10] J.H. Holland, Genetic algorithms and the optimal allocation of trials, SIAM J. Comput. 2 (2) (1973) 88–105, http://dx.doi.org/10.1137/0202009, arXiv:https://doi.org/10.1137/0202009.

[11] P. Stansby, S. Draycott, M4 WEC development and wave basin Froude testing, Eur. J. Mech. B Fluids 104 (2024) 182–193, http://dx.doi.org/10.1016/j.euromechflu.2023.12.007, URL https://www.sciencedirect.com/science/article/pii/S0997754623001802.

[12] A. Kurniawan, H. Wolgamot, C. Gaudin, C. Shearer, P. Stansby, B. Saunders, Numerical modelling in the development of the M4 prototype for Albany, Western Australia, International Conference on Offshore Mechanics and Arctic Engineering, vol. 10: Professor Ian Young Honouring Symposium on Global Ocean Wind and Wave Climate; Blue Economy Symposium; Small Maritime Nations Symposium (2023) http://dx.doi.org/10.1115/OMAE2023-105185, V010T13A010. arXiv:https://asmedigitalcollection.asme.org/OMAE/proceedings-pdf/OMAE2023/86922/V010T13A010/7042080/v010t13a010-omae2023-105185.pdf.

[13] H. Wolgamot, C. Gaudin, P. Stansby, K. Adi, W. Ebeling, I. Penesis, The M4 Wave Energy Demonstration Project: Overview, impact and insight, in: Proceedings of the 16th European Wave and Tidal Energy Conference, 2025.

[14] A. Kurniawan, H. Wolgamot, G. McCauley, M. Zering, P. Stansby, Sea trialling the M4 wave energy converter: Initial hydrodynamic performance insights, in: Proceedings of the 16th European Wave and Tidal Energy Conference, 2025.

[15] D. Howe, B. Raju, C. Lynggard Hansen, H. Wolgamot, A. Kurniawan, J.-R. Nader, C. Shearer, P. Stansby, Basin testing of the 1-2-1 M4 WEC, in: Proceedings of the European Wave and Tidal Energy Conference, Vol. 15, 2023, http://dx.doi.org/10.36688/ewtec-2023-522, URL https://submissions.ewtec.org/proc-ewtec/article/view/522.

[16] J. Apsley, X. Zhang, M. Iacchetti, I.E. Damian, Z. Liao, G. Li, P. Stansby, G. Li, H. Wolgamot, C. Gaudin, A. Kurniawan, X. Zhang, Z. Lin, N. Fernando, C. Shearer, B. Saunders, Integrated hydrodynamic-electrical hardware model for wave energy conversion with M4 ocean demonstrator, in: Proceedings of the European Wave and Tidal Energy Conference, Vol. 15, 2023, http://dx.doi.org/10.36688/ewtec-2023-500, URL https://submissions.ewtec.org/proc-ewtec/article/view/500.

[17] Z. Liao, X. Zhang, J. Apsley, M.F. Iacchetti, P. Stansby, G. Li, A sea-state-dependent control strategy for wave energy converters: Power limiting in large wave conditions and energy maximising in moderate wave conditions, IEEE Trans. Sustain. Energy (2024) 1–11, http://dx.doi.org/10.1109/TSTE.2024.3373121.

[18] J. Tan, H. Polinder, P. Wellens, S. Miedema, The fair evaluation of wave energy converters, in: International Conference on Offshore Mechanics and Arctic Engineering, vol. 9: Ocean Renewable Energy, 2020, http://dx.doi.org/10.1115/OMAE2020-18427, V009T09A016. arXiv:https://asmedigitalcollection.asme.org/OMAE/proceedings-pdf/OMAE2020/84416/V009T09A016/6607297/v009t09a016-omae2020-18427.pdf.

[19] P. Stansby, E. Carpintero Moreno, T. Stallard, Large capacity multi-float configurations for the wave energy converter M4 using a time-domain linear diffraction model, Appl. Ocean Res. 68 (2017) 53–64, http://dx.doi.org/10.1016/j.apor.2017.07.018, URL http://www.sciencedirect.com/science/article/pii/S0141118717302146.

[20] Z. Liao, N. Gai, P. Stansby, G. Li, Control-oriented modelling of wave energy converter M4, in: Asian Wave and Tidal Energy Conference, Taipei, Taiwan, 2018, URL https://tethys-engineering.pnnl.gov/sites/default/files/publications/AWTEC2018-425.pdf.

[21] W.E. Cummins, The impulse response function and ship motions, 1962, URL https://dome.mit.edu/handle/1721.3/49049.

[22] Z. Liao, N. Gai, P. Stansby, G. Li, Linear non-causal optimal control of an attenuator type wave energy converter M4, IEEE Trans. Sustain. Energy (2019) 1, http://dx.doi.org/10.1109/TSTE.2019.2922782.

[23] J. Ukonsaari, R. Vattenfall, N. Bennstedt, Maintenance Effect on Present and Future Gearboxes for Wind Turbines, VattenFall R&D, Autoinvent, Energiforsk, ISBN: 978-91-7673-279-3, 2016.

[24] Boneng, P-Type Planetary Gearbox, Motion Technologies Pty Limited, 2023, available from www.motiontech.com.au by request.

[25] Marine energy cost estimation methodology, 2006, by The Carbon Trust and Entec UK Ltd, available from 'https://www.carbontrust.com/our-work-and-impact/guides-reports-and-tools/marine-energy-cost-estimation'.

[26] E. Hau, Wind Turbines: Fundamentals, Technologies, Application, Economics, third ed., Springer, Berlin, 2013.

[27] G.R. Slemon, X. Liu, Modeling and design optimization of permanent magnet motors, Electr. Mach. Power Syst. 20 (2) (1992) 71–92, http://dx.doi.org/10.1080/07313569208909572, arXiv:https://doi.org/10.1080/07313569208909572.

[28] J. Pyrhonen, T. Jokinen, V. Hrabovcova, Design of Rotating Electrical Machines, John Wiley & Sons, 2013.

[29] P. Stansby, E. Carpintero Moreno, T. Stallard, Capture width of the three-float multi-mode multi-resonance broad-band wave energy line absorber M4 from laboratory studies with irregular waves of different spectral shape and directional spread, J. Ocean Eng. Mar. Energy 1 (3) (2015) 287–298, http://dx.doi.org/10.1007/s40722-015-0022-6, The project is supported by EPSRC through the Supergen Marine Challenge 2 Grant Step-WEC (EP/K012487/1).

[30] L. Sun, J. Zang, P. Stansby, E. Carpintero Moreno, P. Taylor, R. Eatock-Taylor, Linear diffraction analysis of the three-float multi-mode wave energy converter M4 for power capture and structural analysis in irregular waves with experimental validation, J. Ocean Eng. Mar. Energy 3 (1) (2017) http://dx.doi.org/10.1007/s40722-016-0071-5.